Electronic Supplementary Material (ESI) for CrystEngComm.

Facile and Economical Synthesis of ZnS Nanotubes and Their Superior Adsorption Performance for Organic Dyes

Meizhen Guo, Meiyu Song, Shanshan Li, Zhilei Yin, Xinyu Song*, YuxiangBu

School of Chemistry and Chemical Engineering, Shandong University,

Jinan, 250100, P. R. China

Supplementary Materials

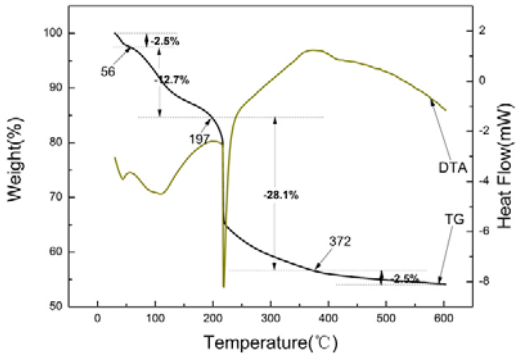

Fig. S1. TG and DTA curves of rod-like precursors

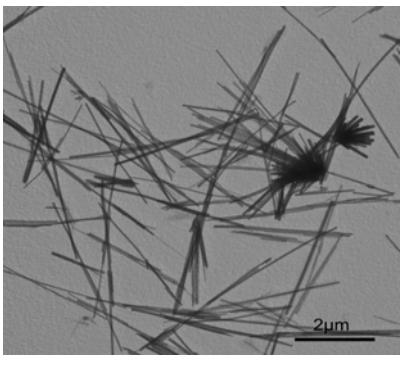

Fig. S2. Zn-precursors prepared with 20 mL water.

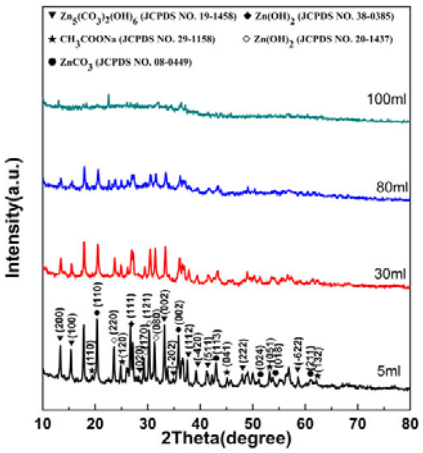

Fig. S3. XRD of precursor prepared with different water amount: 5 mL, (b) 30 mL, (c) 80 mL, (d) 100 mL.

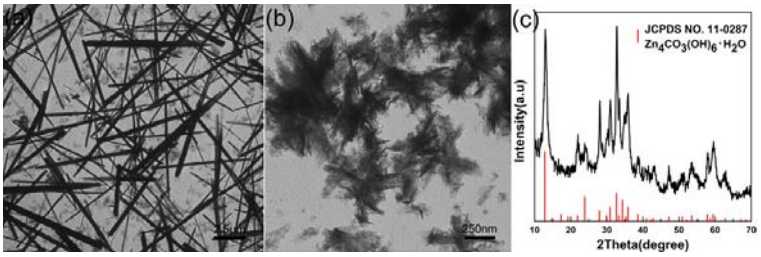

Fig. S4. Zn-precursors after washing with different solvent under ultrasonic condition: (a) alcohol, (b) water, (c) XRD of the precursor after washing with water.

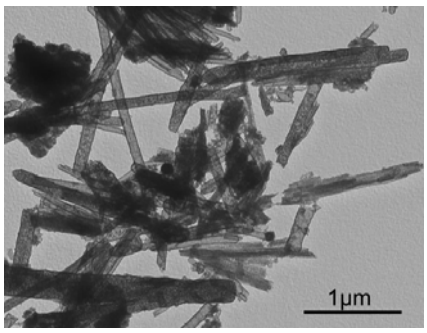

Fig. S5. TEM image of the nanotubes formed under stirring.

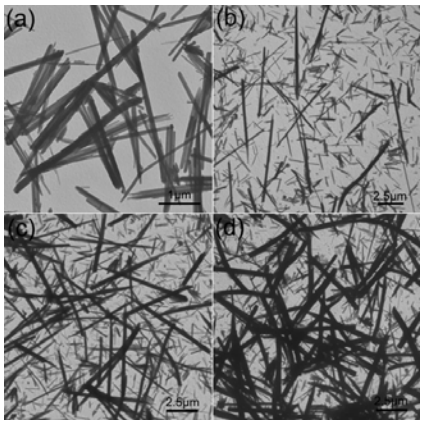

Fig. S6. TEM images of the rod-like precursors produced at different mole ratio of reactants ($Zn(CH_3COO)_2$: $NaHCO_3$): (a) 1:1, (b) 1:1/2, (c)1:1/4 (d)1:1/6.

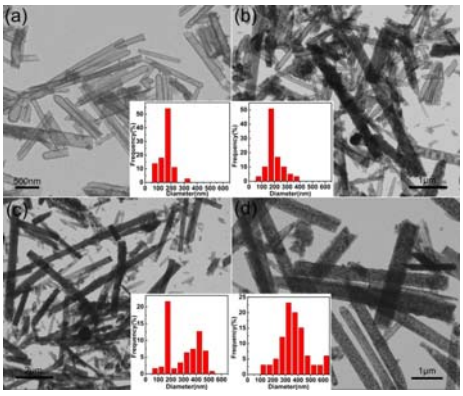

Fig. S7. TEM images of ZnS nanotubes synthesized with a mole ratio of $Zn(CH_3COO)_2$ to $NaHCO_3$: (a)1:1, (b) 1: 1/2, (c) 1:1/4, (d) 1:1/6. The inset is the diameter distribution histogram of the nanotubes obtained from corresponding TEM image.

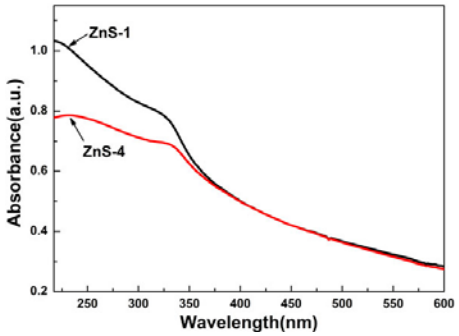

Fig. S8. UV-vis absorption spectrum of ZnS-1 and ZnS-4 nanotubes.

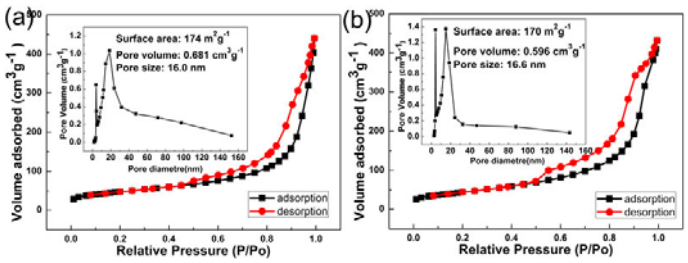

Fig. S9. Typical N_2 adsorption–desorption isotherm and pore-size distribution curve of the nanotubes: (a) ZnS-1, (b) ZnS-4.

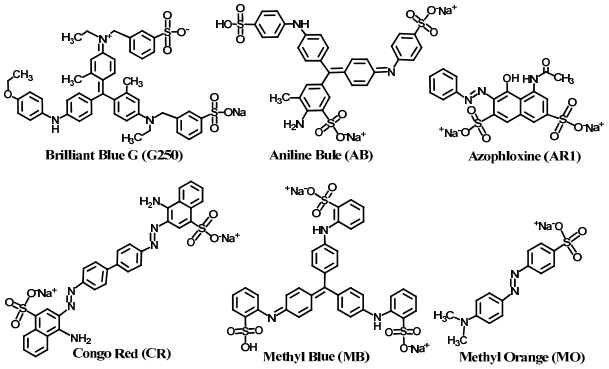

Fig. S10. The molecular structures of the dyes used in adsorption.

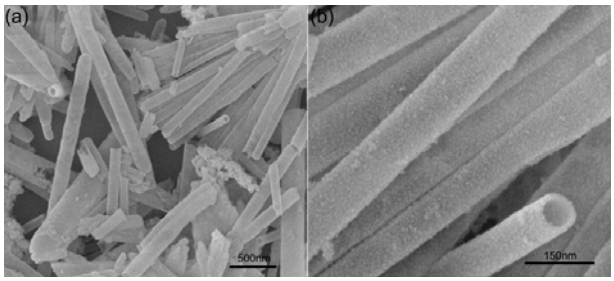

Fig. S11. SEM images of ZnS-1 nanotubes after the CR dye adsorption experiments.

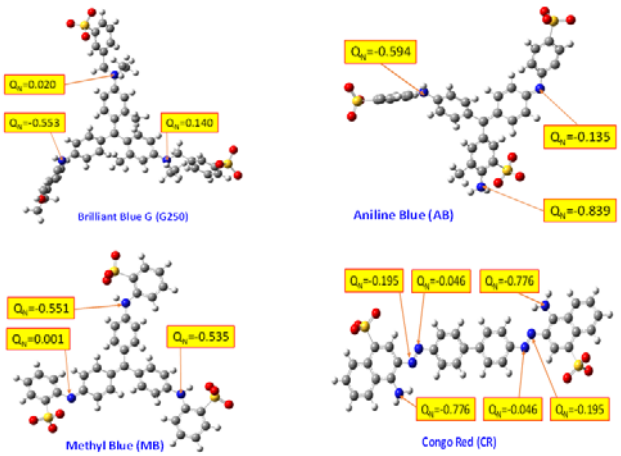

Fig. S12. The optimized structures of 4 dye molecules and calculated Mulliken charge densities of N atoms (Q_N) in each dye molecule at the B3LYP/6-31+G* level.

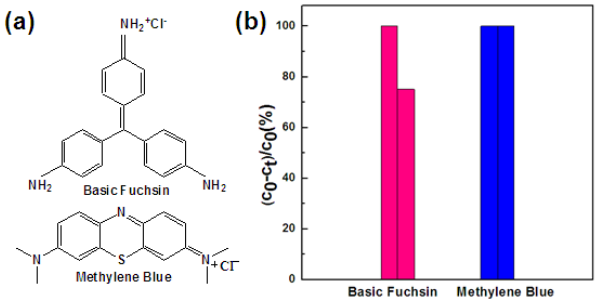

Fig. S13. (a) Molecular structure of basic fuchsin and methylene blue, respectively. (b) The absorption efficiency of basic fuchsin and methylene blue before (left) and after (right) adsorption on ZnS nanotubes, respectively.

Table S1. Fitting Parameters for Langmuir and Freundlich isotherm model.

	Langmuir model			Freundlich model		
	q_m (mg g^{-1})	K_L (L mg^{-1})	R^2	K_F (L g^{-1})	n_F	R^2
ZnS-1	724.6	0.9388	0.9996	353.2	4.778	0.7085
ZnS-2	751.9	0.7733	0.9995	351.3	4.493	0.7068
ZnS-3	757.6	1.4642	0.9980	447.0	6.103	0.3585
ZnS-4	793.6	0.9692	0.9986	381.1	4.251	0.6547

Table S2 Comparison of available adsorption capacities of some composite adsorbents for adsorption of CR

sample	q_m (mg g^{-1})	reference
MgO–$MgFe_2O_4$ composite	498	48
Graphene oxide–chitosan/silica	294	47
Magnetite@graphene	33.66	86a
Hollow α-Fe_2O_3 and Fe_2O_3 nanowires	93.5 and 84.5	86b
Co_3O_4–Fe_3O_4 tripple-shelled spheres	125	87a
Fe/FeOOH	167.8	87b
hollow aluminosilica microsphere@hierarchical g-AlOOH/$Fe(OH)_3$	252.53	46
Ni doped ZnS nanoparticles loaded on activated carbon (Ni-ZnS-NP-AC) and Pd nanoparticles loaded on activated carbon (Pd-NP-AC)	286 and 126.6	41
ZnS nanotubes	724.6	This work

Table S3. Pseudo-first-order model and Pseudo-second-order model parameter

		Pseudo-first-order			Pseudo-second-order		
	$q_{e,exp}$ (mg g^{-1})	q_{e1} (mg g^{-1})	K_1 (min^{-1})	R^2	q_{e2} (mg g^{-1})	K_2 (g mg^{-1} min^{-1})	R^2
ZnS-1	247.2	52.38	0.010	0.8628	246.9	1.5×10^{-3}	0.9996
ZnS-2	245.0	65.52	0.008	0.9222	239.8	1.1×10^{-3}	0.9991
ZnS-3	245.6	61.32	0.011	0.9250	247.5	1.1×10^{-3}	0.9994
ZnS-4	245.9	117.4	0.010	0.9834	248.1	4.9×10^{-4}	0.9944

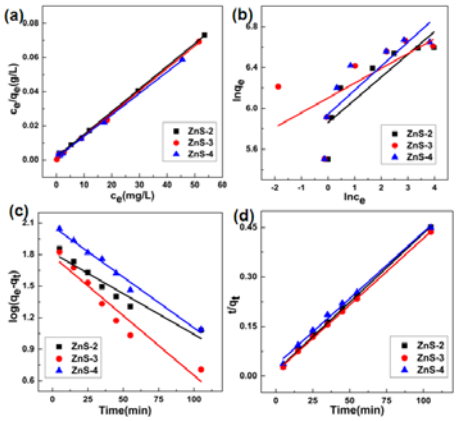

Fig. S14. Adsorption isotherm and kinetics models fitted to experimental data for the adsorption of CR (50-200 mg/L) by 10 mg ZnS-2, ZnS-3 and ZnS-4, respectively (a) Langmuir model, (b) Freundlich isotherm model, (c) Pseudo-first-order, (d) Pseudo-second-order kinetics model.

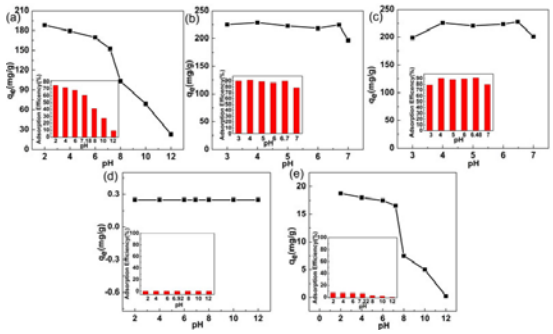

Fig. S15. Effect of initial pH of several dyes (50 mg/ L) on adsorption capacity (q_e) and efficiency of ZnS nanotubes (10 mg). (a) G250, (b) AB, (c) MB, (d) MO, (e) AR1.

As demonstrated in Fig. S16, 10 mg nanotubes ZnS into CR dye solutions with different concentration without adjusting pH at room temperature, the dye was almost completely adsorbed after adsorption equilibrium. Therefore, we selected MO dye to carry out the photocatalytic performances due to the weak adsorption ability of the ZnS nanotubes towards MO. The experimental result is given in Fig. S17

The experimental result demonstrates that the degradation efficiency of ZnS nanotubes to MO reached about 89%, which is higher than that of P25 and many pure ZnS nanomaterials reported in literatures. Some reported ZnS materials for MO

degradation in literatures are listed in Table S4. However, the obtained ZnS nanotubes do not show higher photocatalytic efficiency to MO compared to those ZnS composites, such as g-C_3N_4/ZnS (*Eur. J. Inorg. Chem*., 2015, 24, 4108-4115. ZnS /chitosan ***(****Appl. Catal. B: Environ. 2014, 158–159, 269–279*). This may be related to the high defects in the as-prepared ZnS nanotubes. It was reported that good crystalline quality and low concentration of defects are beneficial for increasing photocatalytic activity, because of lower losses of photogenerated carriers. (*J. Phys. Chem. C*, ***2011****, 115, 11095–11101. J. Phys. Chem. C 2011, 115, 13844−13850.)*

Fig. S16. Image of adsorption of CR before and after using ZnS Nanotubes as adsorbent. (10 mg ZnS-1)

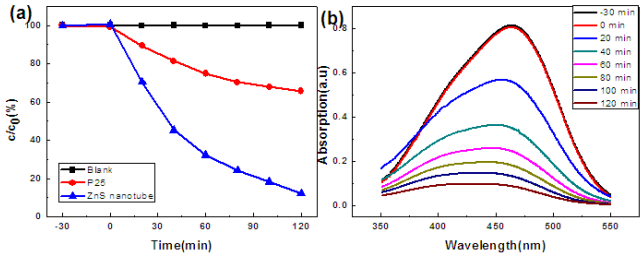

Fig. S17. (a) Photocatalytic degradation of MO (10 mg/L) under visible light irradiation at 25℃ with ZnS nanotubes, (b) Absorption spectrum of MO with irradiation time in presence of ZnS nanotubes.

Table S4. The Degradation Effect of Different ZnS or ZnS-based Photocatalysts Reported in the Following references

Type of catalysts	Light source (Decomposing MO)	Pollutants (ρ/V) (mg • L^{-1}/mL)	Catalysts (mg)	Results	Ref.
pure ZnS	Ultraviolet light	10/100	50	DP of 54% after 2h	1
ZnS nanoparticles	Ultraviolet light	10/100	50	DP of 95% after 2h	2
ZnS hollow sphere and ZnS nanocrystal	Ultraviolet light	20/100	150	DP of 95% after 5.8h	3
ZnS nanoparticles	Ultraviolet light	10/20	10	DP of 47% after 2h	4
ZnS/ESM composites	Ultraviolet light	10/300	300	DP of ＜85% after 2h	5
MWCNT/ZnS heterostructures	Ultraviolet light	20/100	150	DP of ＜85% after 2h	6
P25	Ultraviolet light	10/50	10	DP of 34% after 2h	This work
ZnS nanotubes	Ultraviolet light	10/50	10	DP of 88% after 2h	This work

1 F. J. Chen，Y. L. Cao，D. Z. Jia and A. J. Liu，*Dyes Pigments*, 2015, **120**, 8–14.

2 F. J. Chen, Y. L. Cao and D. Z. Jia, *Ceram. Int.*, 2015, **41**, 6645–6652.

3 L. H. Dong, Y. Chu, Y. P. Zhang, Y. Liu and F. Y. Yang, *J. Colloid Interf. Sci.*, 2007, **308**, 258–264.

4 F. J. Chen, Y. L. Cao and D. Z. Jia, *CrystEngComm*, 2013, **15**, 4747–4754.

5 G. H. Zhang, C. H. Li, X. D. Zhang, X. Guo, Y. C. Liu, W. Y. He, J. R. Liu, H. Wang and Y. F. Gao, *RSC Adv*., 2014, **4**, 13569–13574.

6 H. Q. Wu, Q. Y. Wang, Y. Z. Yao, C. Qian, X. J. Zhang and X. W. Wei, *J. Phys. Chem. C*, 2008, **112**, 16779–16783.